

Supplemental Figures

Figure S1. In vitro cell growth inhibition assay with DXd.

Figure S2. Enhanced cytokine production by tumor-infiltrating immune cells by U3-1402 treatment.

Figure S3. Individual survival curves from the CD8⁺ cells depletion experiment.

Figure S4. In vivo antitumor efficacy and ex vivo re-stimulation assay with DXd.

Figure S5. Antitumor effect of anti-PD-1 and U3-1402 therapy, and expression levels of effector/proliferation markers when the tumor burden is low.

Figure S6. In vivo treatment efficacy of U3-1402 and PD-1 inhibitor, and the characteristics of mouse HER3-expressing cancer cells.

Figure S7. Intra-tumoral MDSCs and Tregs density.

Figure S8. Enhanced cytokine production by tumor-infiltrating immune cells after combo treatment.

Figure S9. Evaluation of HER3 expression in immune cells.

Figure S10. Induced infiltration of myeloid cells and NK cells with U3-1402 treatment, and evaluation of TLR4 expression in intra-tumoral immune cells.

Figure S11. Representative figures for each immunohistochemical HER3 score.

Figure S12. OS curves based on HER3 positivity in the entire patient population, and HER3 scores of PD-1 inhibitor responders.

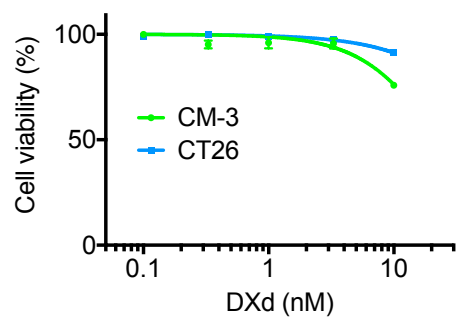


Figure S1. In vitro cell growth inhibition assay with DXd.

Data represents the means \pm SEM of six replicates, and are representative of two independent experiments.

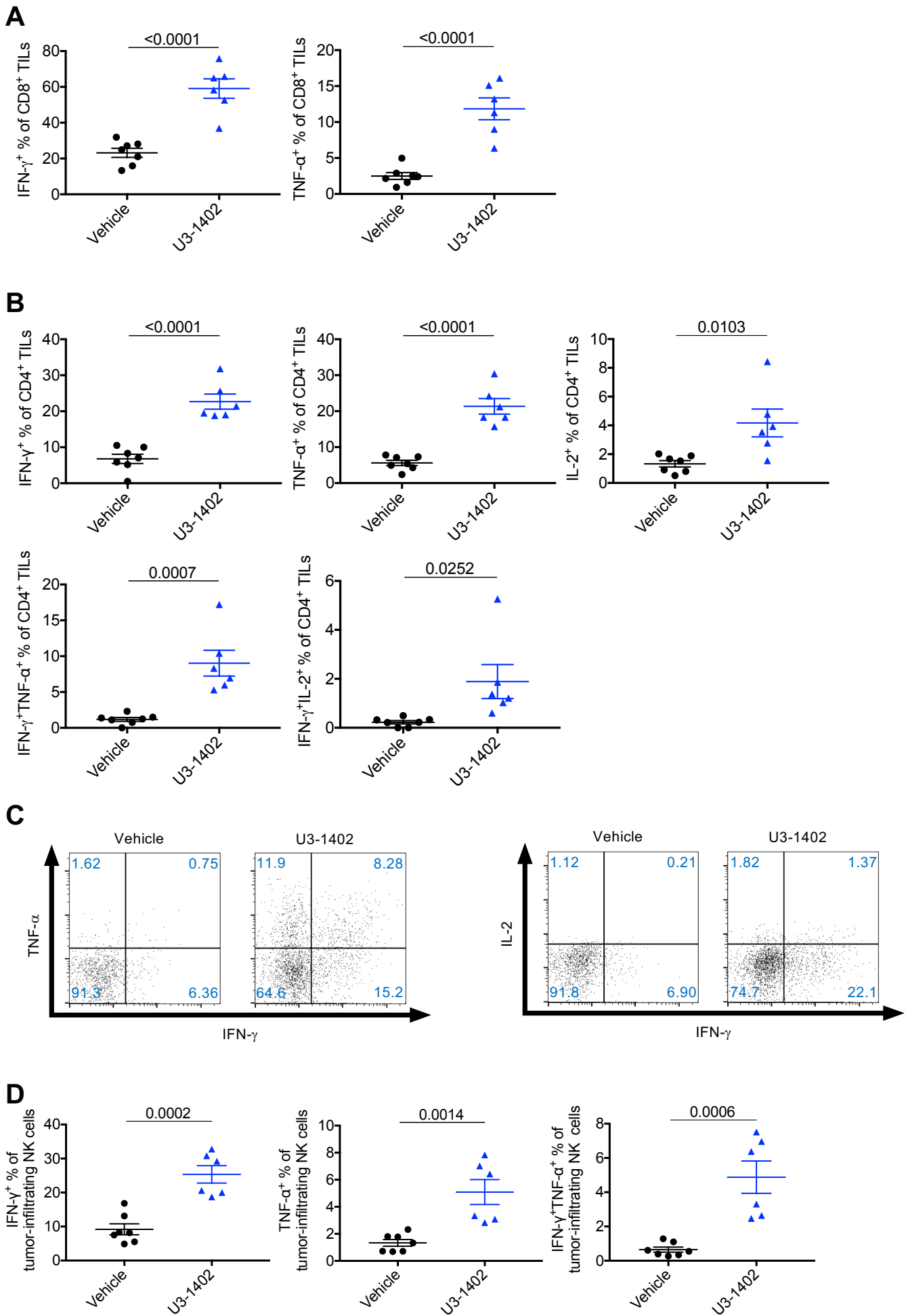


Figure S2. Enhanced cytokine production by tumor-infiltrating immune cells by U3-1402 treatment.

(A, B and D) Flow cytometry analysis of the indicated cell types. Each dot represents one tumor. $n = 6-7$ for each arm. The P values are shown on horizontal lines. Data were assessed by unpaired t-test. (C) Representative images of interferon- γ (IFN- γ) and tumor necrosis factor- α (TNF- α) producing CD4⁺ tumor-infiltrating lymphocytes (TILs) (left), and IFN- γ and interleukin-2 (IL-2) producing CD4⁺ TILs (right). Each value in the figures indicates the frequency of each cell type. NK, natural-killer.

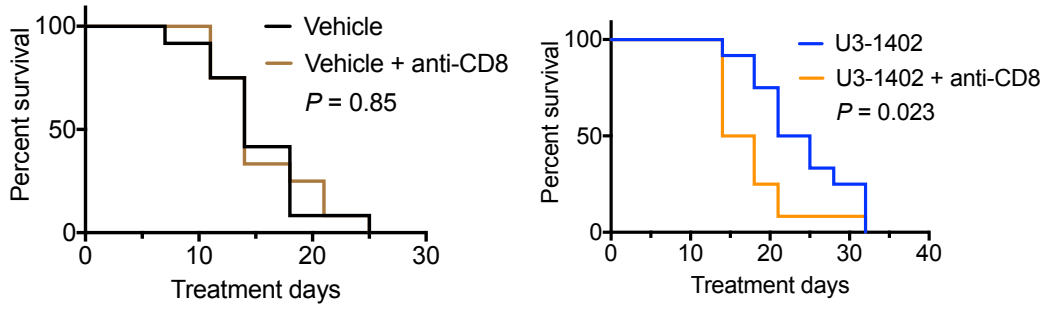


Figure S3. Individual survival curves of CD8⁺ cells depletion experiment.

$n = 12$ for each arm, pooled from 4 independent experiments. The treatment was initiated when tumor sizes reached 80–250 mm³ (high tumor burden). CD8⁺ cell depletion weakened U3-1402 treatment efficacy (right) although it did not affect natural tumor growth (left). Differences in survival curves were assessed using a log-rank test.

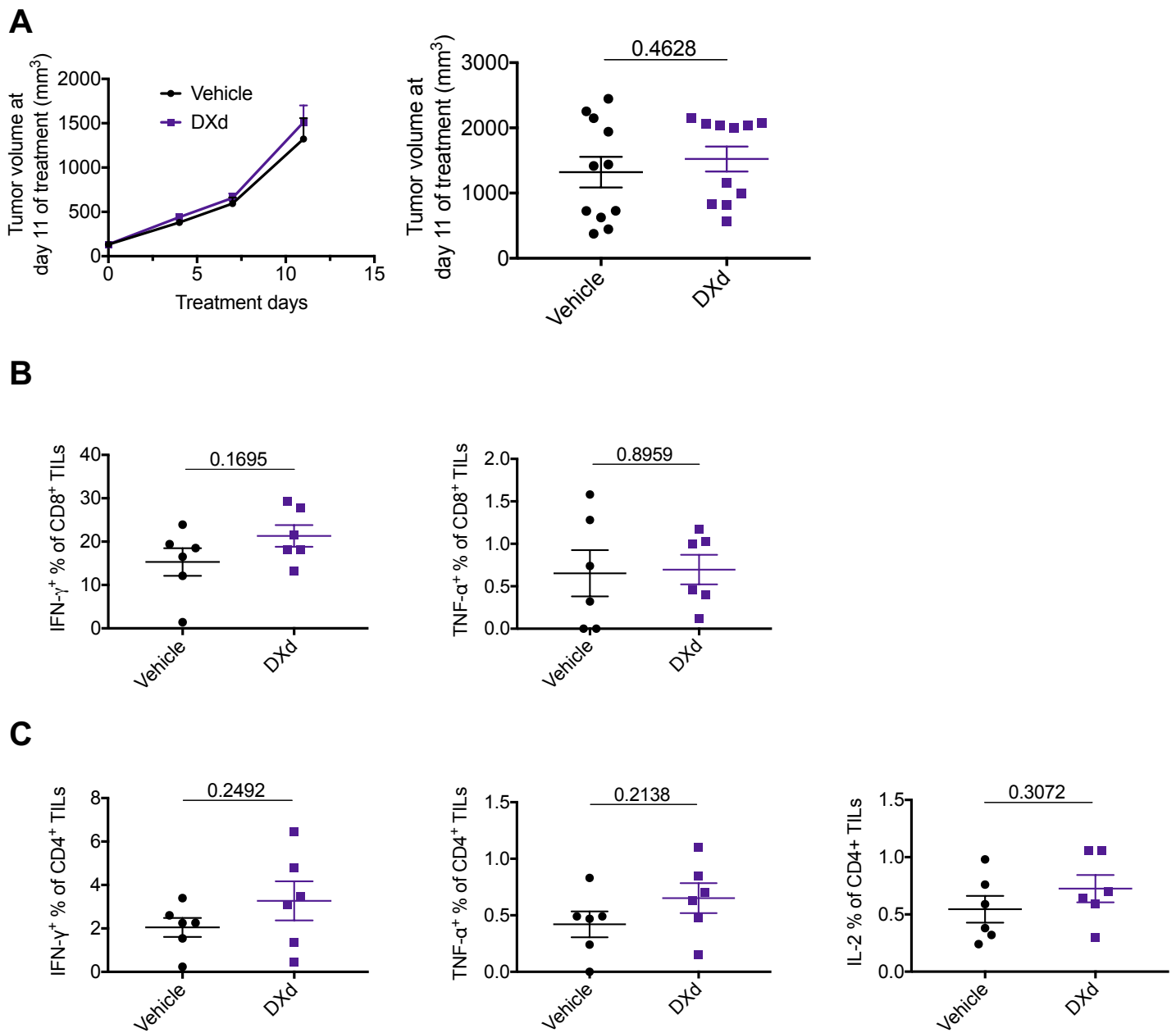


Figure S4. In vivo antitumor efficacy and Ex vivo re-stimulation assay with DXd.

(A) Left: Tumor volume curve of subcutaneous CM-3 tumors. The treatment was initiated when tumor sizes reached 80–250 mm³. Right: Tumor volume 11 days after treatment initiation. $n = 11$ for each arm, pooled from two independent experiments. (B) Flow cytometry analysis of CD8⁺ tumor-infiltrating lymphocytes (TILs). $n = 6$ for each arm. (C) Flow cytometry analysis of CD4⁺ TILs. $n = 6$ for each arm. Each dot in A–C represents one tumor. The P values in A–C are shown on horizontal lines. Data were assessed by unpaired t-test. IFN- γ , Interferon- γ . TNF- α , Tumor necrosis factor- α . IL-2, interleukin-2.

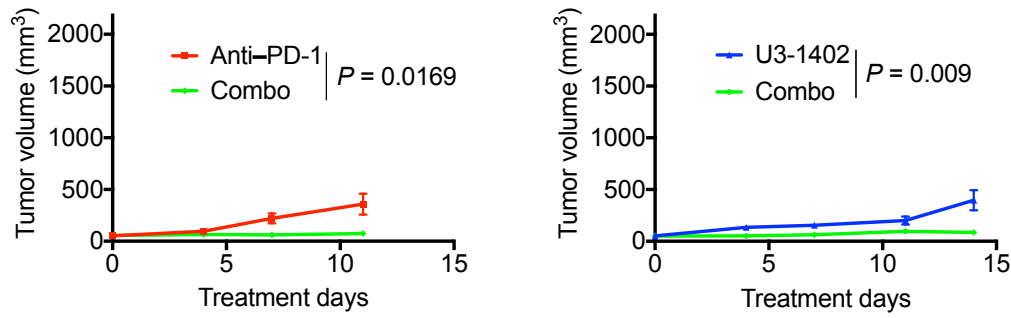
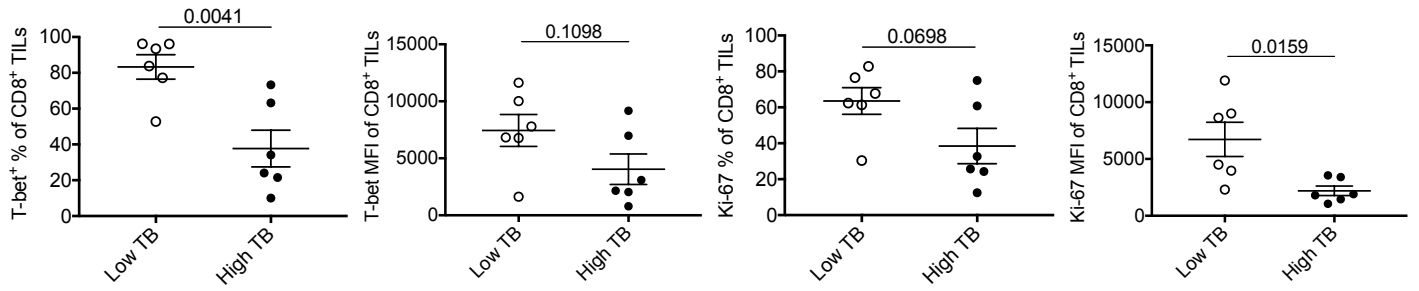
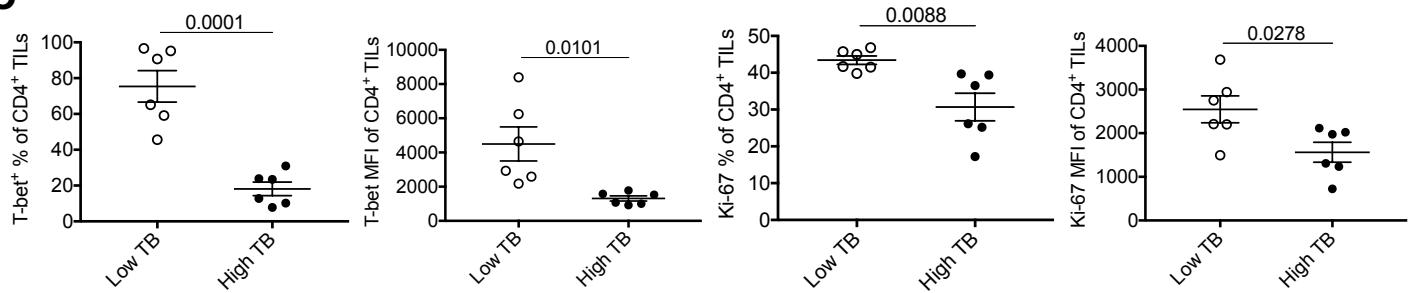
A**B****C**

Figure S5. Antitumor effect of anti-PD-1 and U3-1402 therapy, and expression levels of effector/proliferation markers when the tumor burden is low.

(A) Tumor volume curve of subcutaneous CM-3 tumors. $n = 7$ for each arm, pooled from two independent experiments. The P values are shown on the right side of vertical lines. Data were assessed by unpaired t-test. The treatment was initiated when tumor sizes reached 40–80 mm³. These experiments were performed independently of those shown in Figure 2. The tumor volume curves were plotted until the first observed death. (B and C) Flow cytometry analysis of the indicated cell types based on tumor burdens (TBs). Low TB, 40–80 mm³. High TB, 80–250 mm³. $n = 6$ for each arm. The P values are shown on horizontal lines. Data were assessed by unpaired t-test. PD-1, programmed cell death-1. TILs, tumor-infiltrating lymphocytes. MFI, mean fluorescent intensity.

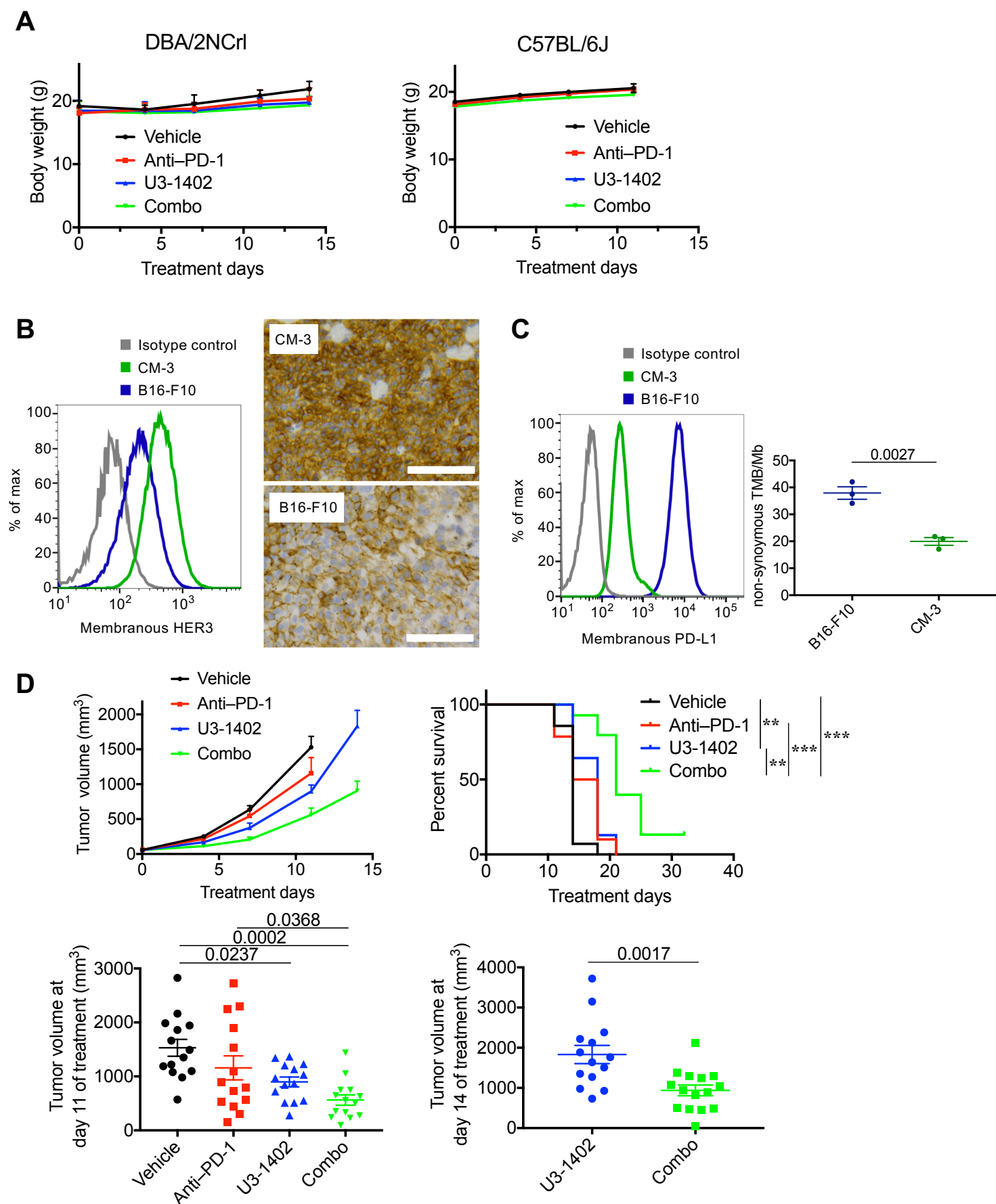
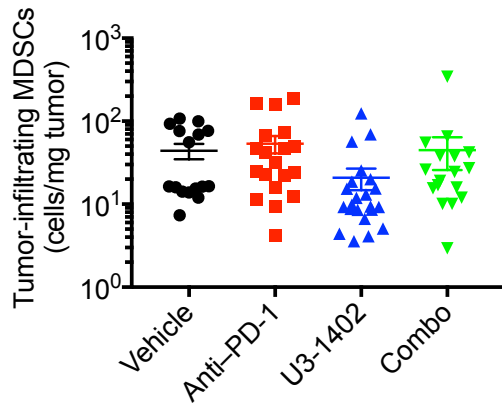
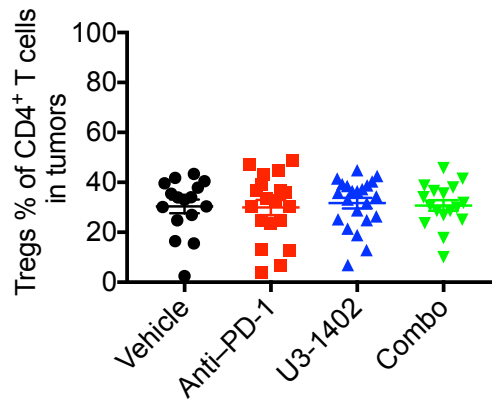


Figure S6. In vivo treatment efficacy of U3-1402 and PD-1 inhibitor, and the characteristics of mouse HER3-expressing cancer cells. (A) Body weight changes of mice during treatment. Left: $n = 11$ for each arm, pooled from four independent experiments with DBA/2NCRl mice carrying CM3 tumors. The treatment was initiated when tumor sizes reached 80–250 mm³. Right: $n = 14$ for each arm, pooled from two independent experiments with C57BL/6J mice carrying B16-F10 tumors. The treatment was initiated when tumor sizes reached 20–80 mm³. (B) Flow cytometry analysis of membranous HER3 expression of cultured cells. Images of membranous HER3 immunostaining of CM-3 tumor (top) and B16-F10 tumor (bottom). Scale bars, 100 μ m. Data and figures are representative of three independent experiments. (C) Left: Flow cytometry analysis of membranous programmed cell death-ligand 1 (PD-L1) expression. Data are representative of three independent experiments. Right: Non-synonymous tumor mutation burden (TMB) from whole exome sequencing analysis of fresh frozen tumor tissue. (D) Top: Tumor volume curve of subcutaneous B16-F10 tumors (left) and survival curve of B16-F10 tumor-carrying mice (right) treated as indicated. Bottom: Tumor volume at 11 days (left) or 14 days (right) after treatment initiation. $n = 14$ for each arm, pooled from two independent experiments. The P values are shown on horizontal lines only when they were < 0.05 . ** or *** indicates P values < 0.01 or < 0.001 , respectively. Data were assessed by unpaired t-test (C and D) or one-way ANOVA with Tukey's correction for multiple comparisons (D). Differences in survival curves were assessed using a log-rank test (D). PD-1, programmed cell death-1.

A**B****Figure S7. Intra-tumoral MDSCs and Tregs density.**

Flow cytometry analysis of the indicated cell types. Each dot represents one tumor. $n = 16-22$ for each arm, pooled from five independent experiments. MDSCs, myeloid-derived suppressor cells. Tregs, regulatory T cells. PD-1, programmed cell death-1.

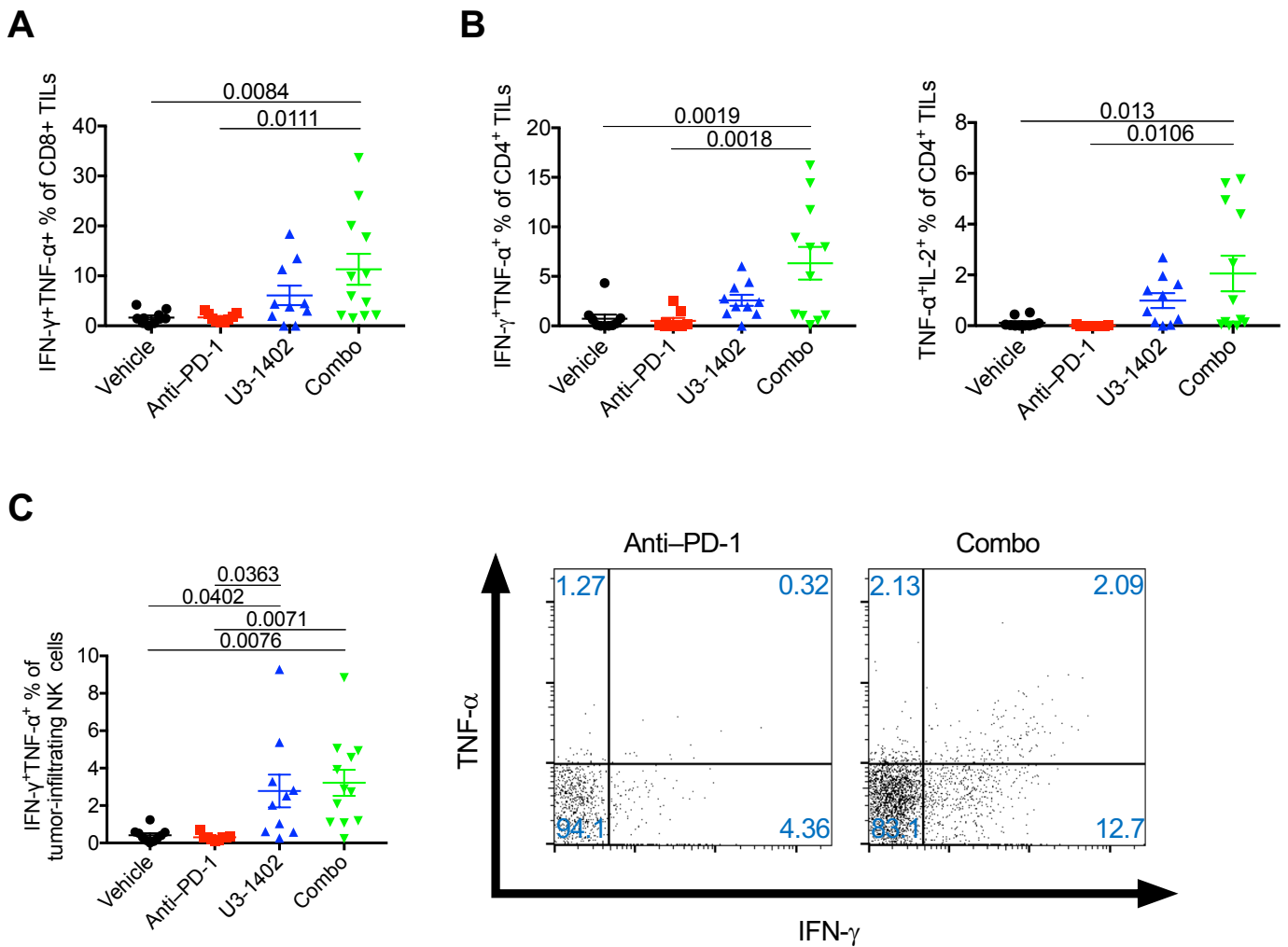


Figure S8. Enhanced cytokine production by tumor-infiltrating immune cells after combo treatment.

(A and B) Flow cytometry analysis of the CD8⁺ (A) and CD4⁺ (B) tumor-infiltrating lymphocytes (TILs). Each dot represents one tumor. $n = 9-10$ for each arm. The P values are shown on horizontal lines only when they were < 0.05 in multiple comparisons. Data were assessed by one-way ANOVA with Tukey's correction for multiple comparisons. (C) Left: Flow cytometry analysis of the tumor-infiltrating natural killer (NK) cells. Each dot represents one tumor. $n = 9-10$ for each arm. The P values are shown on horizontal lines only when they were < 0.05 in multiple comparisons. Data were assessed by one-way ANOVA with Tukey's correction for multiple comparisons. Right: Representative images of interferon- γ (IFN- γ) and tumor necrosis factor- α (TNF- α) producing tumor-infiltrating NK cells. Each value in the figures indicates the frequency of each cell type. PD-1, programmed cell death-1. IL-2, interleukin-2

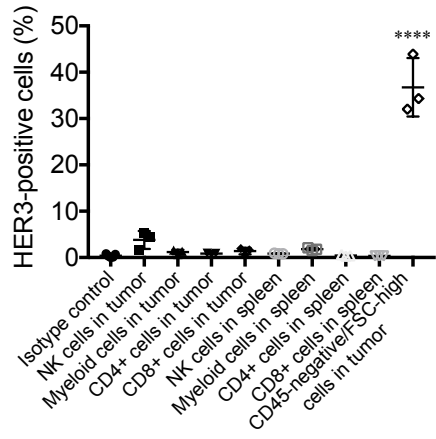
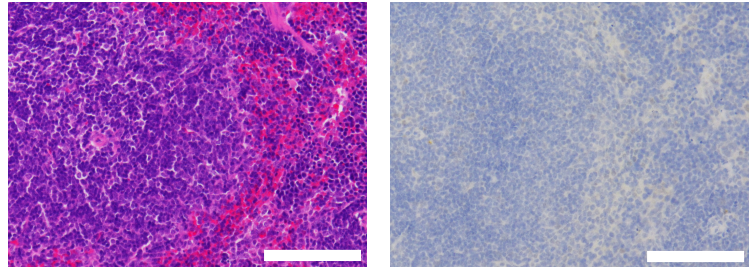
A**B**

Figure S9. Evaluation of HER3 expression in immune cells.

(A) Flow cytometry analysis of HER3 expression in the indicated cell types. $n = 3-5$ for each cell type. There are significant differences in HER3 expression between intra-tumoral CD45-negative/FSC-high cells including CM-3, and each immune cell in both tumors and the spleen (each P value is < 0.0001 in multiple comparisons: ****). (B) Representative images of mouse spleen staining. Left: Hematoxylin-eosin stain. Right: HER3 immunostaining. Scale bars, 100 μm . NK, natural killer. FSC, forward scatter. Data were assessed by one-way ANOVA with Tukey's correction for multiple comparisons.

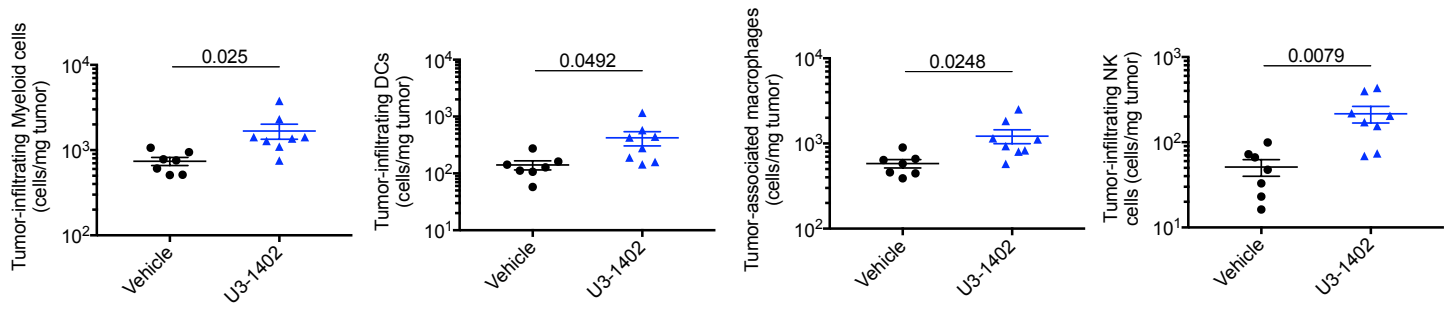
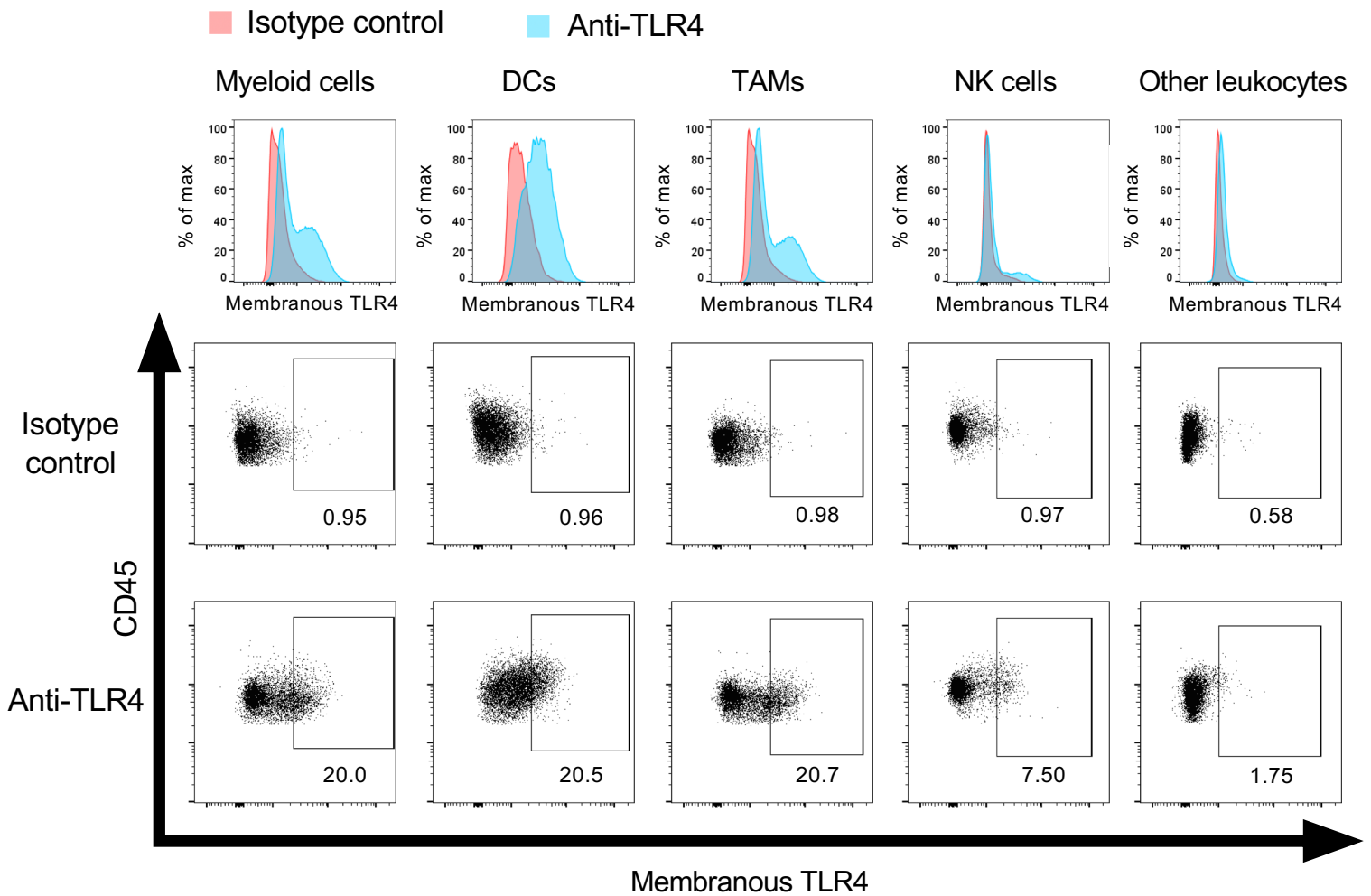
A**B**

Figure S10. Induced infiltration of myeloid cells and NK cells with U3-1402 treatment, and evaluation of TLR4 expression in intra-tumoral immune cells.

(A) Flow cytometry analysis of the indicated cell types. Each dot represents one tumor. $n = 7-8$ for each arm. The P values are shown on horizontal lines. Data were assessed by unpaired t-test. (B) Flow cytometry analysis of membranous toll-like receptor 4 (TLR4) expression in the indicated cell types. Top: Histograms of fluorescence intensity of phycoerythrin (PE). Blue and red curves indicate the histograms of cells stained by PE-conjugated anti-TLR4 antibody and PE-conjugated isotype control antibody. Bottom: Scatter plots of the cells stained by the anti-TLR4 antibody or the corresponding isotype control antibody. Values in the figures indicates the frequency of TLR4⁺ cells which was defined as phycoerythrin (PE)-positive cells. DC, dendritic cell. TAM, tumor-associated macrophage. NK, natural killer.

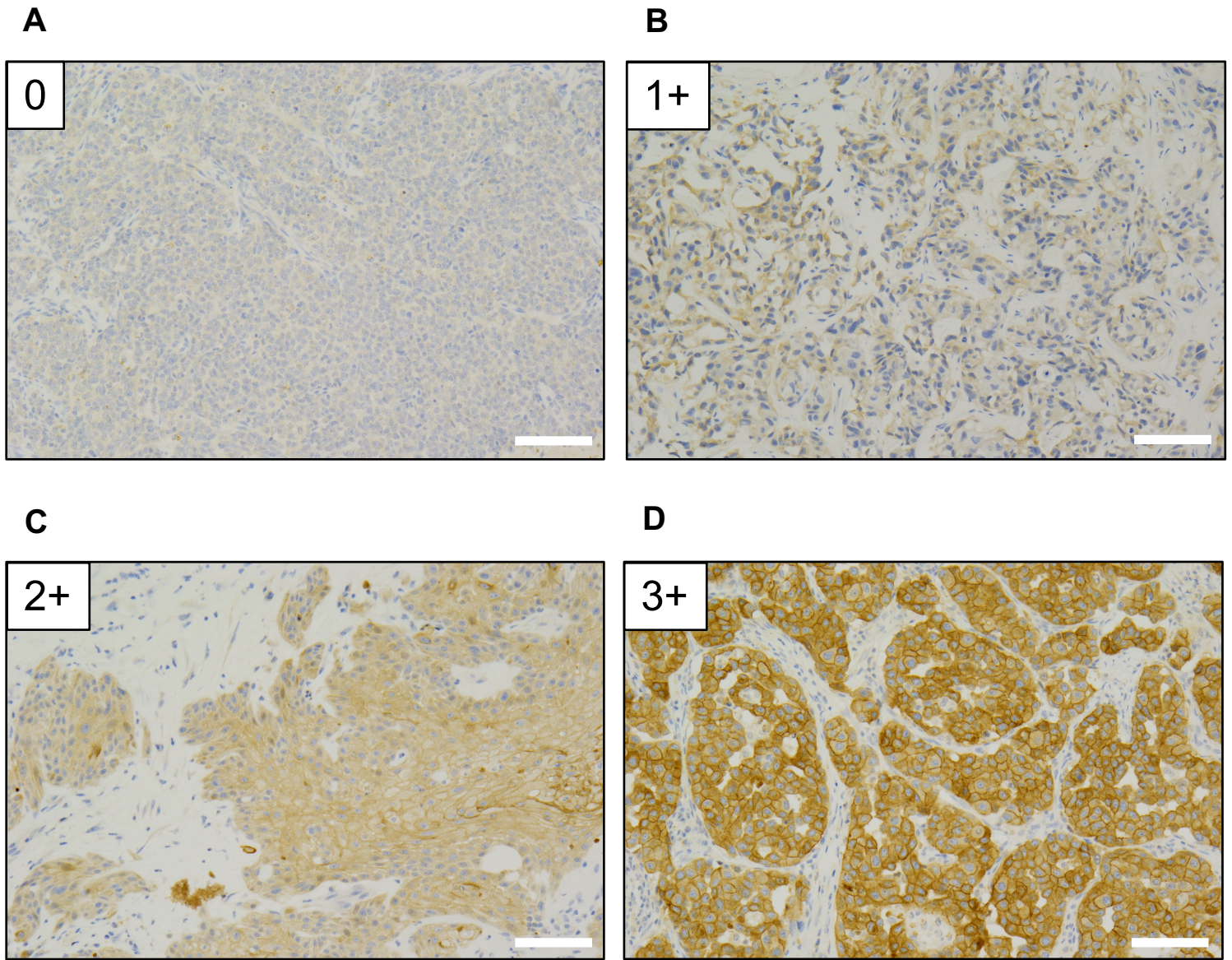


Figure S11. Representative figures for each immunohistochemical HER3 score.

HER3 staining was categorized by intensity as 0, 1+, 2+, and 3+. (A) 0, no staining or membrane staining in $\leq 10\%$ of the tumor cells; (B) 1+, a faint or barely perceptible incomplete membrane staining in $> 10\%$ of tumor cells; (C) 2+, weak-to-moderate complete membrane staining observed in $> 10\%$ of tumor cells; (D) 3+, circumferential membrane staining that is complete, intense, and in $> 10\%$ of tumor cells. Scale bar, 100 μm .

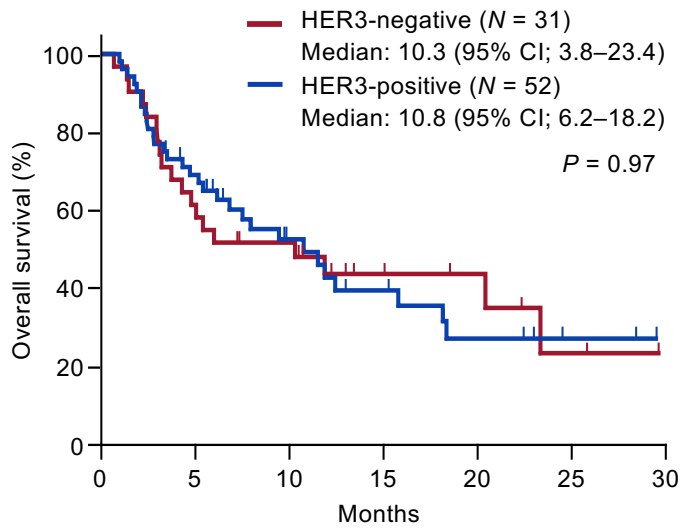
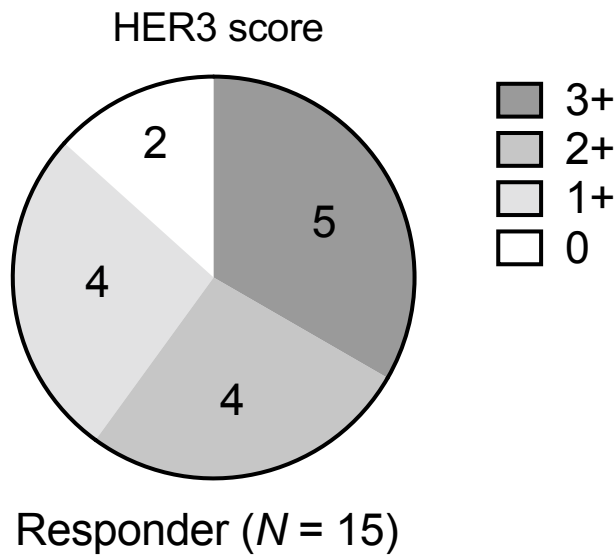
A**B**

Figure S12. OS curves based on HER3 positivity in the entire patient population, and HER3 scores of PD-1 inhibitor responders. (A) Kaplan-Meier curves for overall survival (OS) in HER3-positive or HER3-negative patients treated with programmed cell death-1 (PD-1) inhibitors. Vertical bars denote censoring. CI, confidence interval. A Difference in survival curves was assessed using a log-rank test. (B) Immunohistochemical HER3 scores of tumor tissue of responders to PD-1 inhibitor treatment.